Bulletin of the Seismological Society of America, Vol. 85, No. 6, pp. 1867–1872, December 1995

Short Notes

Frequency Distribution of Geologically Determined Slip Rates for Normal Faults in the Western United States

by J. P. McCalpin

Abstract Short-term and long-term slip rates are contrasted for 18 well-studied faults in the Basin and Range and Rio Grande rift provinces, over periods ranging from 3000 to 4,000,000 yr. The intrinsic variability of the 62 interval slip rates on these normal faults is assessed by normalizing the long-term slip rate of each fault to 0.1 mm/yr. The cumulative density function of the grouped data predicts that, given a mean net slip rate of 0.12 mm/yr, extreme slip rates with 10% and 5% probability of exceedance are 0.51 and 0.92 mm/yr, respectively. These slip rates are considerably higher than those chosen by an expert panel for the Pajarito Fault, New Mexico, which has a long-term mean slip rate of ca. 0.12 mm/yr.

Introduction

One of the critical parameters for a seismic hazard analysis is the slip rate for seismic fault sources. Many probabilistic seismic hazards analyses use the logic tree approach (Coppersmith and Youngs, 1986; Reiter, 1990). A logic tree is a decision flow path consisting of nodes and branches. Each node represents a fault input parameter (e.g., slip per event, rupture length, recurrence interval) necessary for calculation of hazard. Branching off each node are branches that represent a choice of models or discrete values for fault input parameters (e.g., slip rate = 0.1 or 0.3 mm/yr). Each branch is assigned a probability of being correct. The composite hazard is then computed from all the possible permutations of interconnected branches of the logic tree. Unfortunately, very few faults have yielded measurements of slip rate over different geologic time intervals from which a range of realistic slip rate values and their probabilities of occurrence can be estimated. Instead, choices of slip rates for a given fault are often made in an *ad hoc* manner based on the observed mean slip rate over some (often long) period of geologic time and a subjective feeling for the shape of the probability density function (PDF).

This problem of defining slip rate variability became a subject of discussion during a recent seismic hazards analysis of the Los Alamos National Laboratory in northern New Mexico (Woodward-Clyde, 1993). The main seismic source, the Pajarito Fault, displays fault scarps up to 120-m high across the Bandelier Tuff (1.2 Ma), but smaller fault scarps are absent due to the scarcity of younger deposits along the fault zone. Thus, although a long-term vertical slip rate of 0.1 mm/yr (equivalent to net slip rate of 0.12 mm/yr on a 60°-dipping fault) can be calculated for the past 1.2 Ma, there is no information on how much faster or slower slip rates could have been over shorter time periods (thousands to tens of thousands of years). For analyzing future seismic hazards, it is critical to know how fast a short-term slip rate might be, especially at low probability levels.

Due to the geological and cultural constraints along this fault (some scarps are in a National Monument), we may never be able to directly measure slip rate over geologically short time intervals. However, if we assume that the Pajarito Fault behaves like other normal faults in the Rio Grande rift zone (RGRZ) and the Basin and Range province (BRP) for which we do have variable slip rates, then we can use the larger data set as a proxy to establish probable bounds on the behavior of the Pajarito Fault. My premise is that the long-term behavior of faults of a given type can be characterized by observing the aggregate short-term behavior of many faults of the same type or in the same area. This premise underlies the ergodic substitution of space for time that is widely used in seismology, geology, and hydrology (e.g., Hunter and Mann, 1992). The ergodic hypothesis states that "under certain circumstances sampling in space can be equivalent to sampling through time, and that space-time transformations are permissible as a working tool" (Chorley *et al.*, 1984, p. 32). The ergodic substitution of spatial data for temporal data is strictly justifiable only for similar faults, so I have limited the inventory to normal faults in the western United States that display evidence of multiple late Quaternary faulting events in primarily extensional regimes (Fig. 1).

Variable slip rates on normal faults over geologic time can be estimated from fault scarp heights across landforms of different ages at a site, or from displacements of different age datums in trench exposures. The former data are much

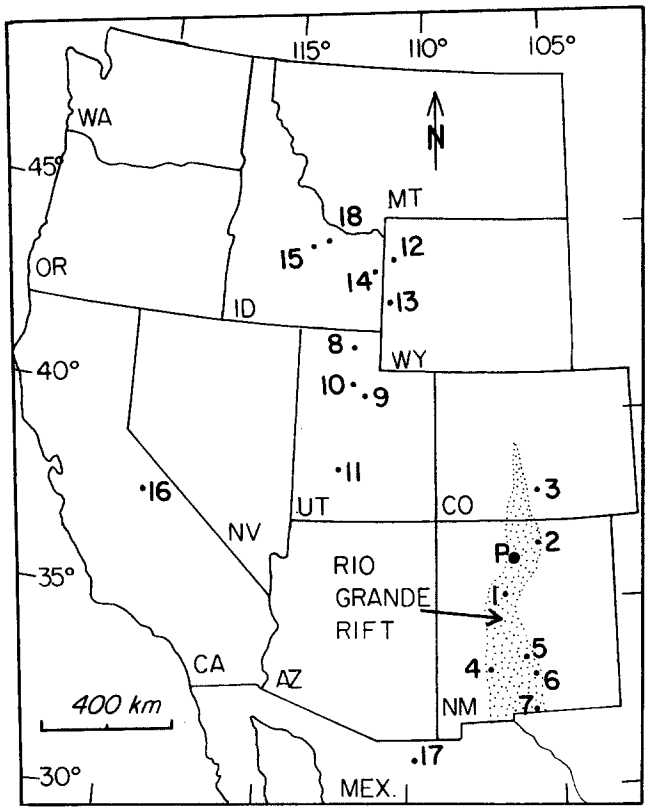

Figure 1. Map of the western United States showing the locations of faults for which slip-rate data are available; numbers are keyed to the site numbers in Tables 1 and 2. Dotted pattern shows the approximate area of the Rio Grande rift; P indicates the Pajarito Fault.

more numerous, but fault scarp heights yield only a measure of vertical separation across the fault. To convert vertical separation to slip or slip-rate values, some assumptions must be made. In this analysis, I assume that (1) any horizontal components of displacement are negligible and (2) on the relatively gentle displaced surfaces, scarp heights are essentially equivalent to the vertical component of fault slip (see McCalpin, 1983). To calculate net slip and net slip rates, one would have to know the dip of each fault in the data set, a parameter that is seldom known with certainty. However, for the purpose of assessing the intrinsic variability in slip rates, it is sufficient to deal with sets of either vertical slip or net slip.

Uncertainties in the inventoried slip rates derived from scarp heights arise from (1) errors in measuring fault scarp heights from topographic profiles, estimated as ±6% to 15% by Mayer (1984, Table 3), and (2) uncertainties in the age of the displaced landform. In practice, almost all of the faulted landforms in this data set (Tables 1 and 2) were dated based on relative dating criteria (particularly soil development) and on correlation to an assumed glacial/interglacial chronology, rather than by numerical ages. Another critical assumption is that the strain accumulated incrementally over the entire life of the landform. For example, if the 120-m-high scarps on the Pajarito Fault were created in the past 600,000 or 300,000 yr instead of the past 1.2 Ma, then slip rates are much higher than estimated.

Discussion

Table 1 lists 34 vertical slip rates from 11 sites on seven faults in the RGRZ, and Table 2 includes 36 vertical slip rates from 14 sites on nine faults in the BRP (Fig. 1). These slip rates span time periods ranging from as little as 3 ky to as much as 4 My. In general, higher slip rates are associated with shorter time intervals (Fig. 2). This association seems to be driven by the highest slip rates, which often represent only a pair of earthquakes closely spaced in time, whereas longer time intervals have a better chance of including long aseismic periods between many earthquakes or clusters of earthquakes.

In order to compare the degree of vertical slip rate variation on numerous faults with different long-term slip rates (ranging from 0.01 to 2.0 mm/yr), the slip rate data must be normalized to a common standard. I chose 0.1 mm/yr as the standard because that value is an average rate for the majority of Quaternary normal faults in the Basin and Range province (dePolo, 1994) and it approximates the long-term slip rate of the Pajarito Fault. The normalization factor (*N* factor) in Tables 1 and 2 is the factor by which a site's long-term slip rate must be multiplied to normalize it to 0.1 mm/yr. By applying this *N* factor to all of the interval slip rates in the data set, I equalized the fast-slip-rate and slow-slip-rate faults in the data set and can now examine the intrinsic variability in slip rates over geologic time in the entire data set.

The empirical frequency distribution of net slip rates for the RGRZ and BRP (assuming a fault dip of 60°) are shown in Figure 3. (The vertical slip rates from Tables 1 and 2 were trigonometrically transformed to equivalent net slip rates merely to permit comparison with the slip estimates of Woodward-Clyde's expert panel). If we accept the ergodic space-for-time substitution, then these curves can be taken as approximating the cumulative density functions (CDF's) of slip rate for a fault with a long-term net slip rate of 0.12 mm/yr. For the RGRZ, net slip rates with 10% and 5% probability of exceedance (i.e., the 90% and 95% cumulative frequency values) are 1.02 and 1.22 mm/yr, respectively. For the BRP, net slip rates with 10% and 5% probability of exceedance are 0.46 and 0.52 mm/yr, respectively. The higher variation in the RGRZ data comes mainly from four anomalously high normalized slip rates (0.72 to 1.65 mm/yr) from the northern Sangre de Cristo and Organ Mountains Faults (Table 1). It is not known if RGRZ faults in general display a higher temporal variation in slip rates than do BRP faults or whether the difference is an artifact of the low number of faults in each province for which data are available. However, the two most detailed paleoseismic studies in the RGRZ (McCalpin, 1983; Machette, 1988) both identified apparent

Table 1
Vertical Slip Rates for Faults in the Rio Grande Rift Zone

Fault Zone	Site*	Reference	Slip Rate (mm/yr)†	Time Period (ka)‡	Long-Term Slip Rate (mm/yr)§	*N* Factor‖	*N* Slip Rate¶
County Dump, Albuquerque, NM	County Dump, **1**	Machette, 1978	0.017 0.12	0–300 300–400	0.04	2.5	0.043 0.30
S. Sangre de Cristo, NM	**2**	Menges, 1990	0.03–0.06 0.12–0.23	0–140 0–4 Ma	0.17	0.588	0.026 0.10
N. Sangre de Cristo, CO	Major Creek, **3**	McCalpin, 1983	0.48 0.43 0.05 0.035	8–13 13–25 25–140 140–400	0.06	1.666	0.80 0.72 0.083 0.058
N. Sangre de Cristo, NM	San Isabel Creek, **3**	McCalpin, 1983	0.24 0.09 0.10 0.09	8–30 30–60 60–140 140–400	0.1	1.0	0.24 0.09 0.10 0.09
N. Sangre de Cristo, NM	Willow Creek, **3**	McCalpin, 1983	0.09 0.38 0.02	8–25 25–35 35–400	0.04	2.5	0.225 0.95 0.05
N. Sangre de Cristo, NM	Uracca Creek, **3**	McCalpin, 1983	0.18 0.04 0.09	8–25 25–140 140–400	0.08	1.18	0.212 0.047 0.106
N. Sangre de Cristo, NM	Blanca Creek, **3**	McCalpin, 1983	0.08 0.01 0.05	15–60 60–140 140–400	0.05	2.0	0.16 0.02 0.10
Caballo, NM	Ash Springs, **4**	Machette, 1987a	0.029 0.044 0.02–0.037	10–125 125–250 250–750	0.035	2.86	0.083 0.126 0.082
San Andres, NM	Central section, **5**	Machette, 1987b	0.018–0.087 0.10–0.18	10–125 125–250	0.105	0.95	0.050 0.133
Organ Mountains, White Sands, NM	Cox Ranch, **6**	Machette, 1987b	1.65 0.43 0.054 0.085	3–5 5–15 15–125 125–250	0.1	1.00	1.65 0.43 0.054 0.085
East Franklin Mountains, El Paso area, NM–TX	Ft. Bliss, **7**	Machette, 1978	0.003 0.064 0.137 0.078	15–125 125–250 250–400 400–750	0.08	1.25	0.004 0.08 0.171 0.098

Statistics for normalized vertical slip rates: $n = 34$, mean = 0.22 mm/yr, standard deviation = 0.34 mm/yr.
*Numbers in bold refer to locations shown on Figure 1.
†Vertical slip rate calculated from the increment of fault scarp height divided by the time period during which that height was created.
‡Time period during which the increment of scarp height was created.
§Total fault scarp height on the oldest datum divided by the age of that datum. This value also equals the weighted average of the slip rates for various time periods at each fault site.
‖*N* factor = normalization factor, derived by dividing the long-term mean vertical slip rate into 0.1 mm/yr.
¶*N* slip rate = vertical slip rate for the given time period multiplied times the *N* Factor for that fault.

temporal clusters of paleoearthquakes separated by long aseismic intervals. Because we do not understand the source of apparent differences in slip-rate variation between the RGRZ and BRP, and because as large a data set as possible is desirable, a CDF-based slip-rate analysis should be performed on a combined RGRZ + BRP data set (62 net slip rates on 16 faults). In the combined all-data set, slip rates with 10% and 5% probabilities of exceedance are 0.51 and 0.92 mm/yr, respectively.

Given the CDF in Figure 3 for "all-fault" data, many possible combinations of discrete slip-rate values and associated probabilities could be placed onto branches in a logic tree. In Figure 4, I contrast the probabilities for the five slip-rate values derived by the consensus of an expert panel (Fig. 4a, from Woodward-Clyde, 1993) to probabilities for the same slip rates as indicated by the CDF (Fig. 4b). The experts had assigned the highest probabilities to slip rates near the mean, and low (10%) probabilities to extremes of slip rate.

Table 2
Vertical Slip Rates for Normal Faults in the Basin and Range Province

Fault Zone	Site*	Reference	Slip Rate (mm/yr)**	Time Period (ka)†	Long-Term Slip Rate (mm/yr)‡	*N* Factor§	*N* Slip Rate‖
Wasatch, UT, Brigham City segment¶	Jim May Canyon, **8**	Machette *et al.*, 1992, Figure 21	0.75 0.33 8.0 0.11	6–10 10–13 13–14 14–170	0.2	0.5	0.375 0.165 4.0 0.055
Wasatch, Provo segment¶	Hobble Creek, **9**	Machette *et al.*, 1992, Figure 21	0.5 6.25	6–14 14–18	2.27	0.044	0.022 0.275
Wasatch, Provo segment¶	Dry Creek, **9**	Machette *et al.*, 1992, Figure 21	5.0 0.21	18–19 19–140	0.21	0.476	2.38 0.01
West Valley, UT	Granger Fault, **10**	Machette *et al.*, 1992, Figure 21	0.15 0.062	13–60 60–140	0.13	0.77	0.116 0.048
Beaver, UT	Beaver Fault, **11**	Machette, 1985, p. 34	0.067 0.040	15–150 150–500	0.05	2.0	0.134 0.08
Teton, WY	Signal Mtn., **12**	Pierce and Morgan, 1992	1.33 1.25 0.0625–1.09	0–15 ka 0–2 Ma 2–6 Ma	1.25	0.08	0.106 0.10 0.069
Star Valley, WY	Afton, **13**	McCalpin, 1993	1.53 0.54	5.5–8.1 8.1–15.5	0.71	0.14	0.214 0.076
Grand Valley, ID	**14**	Pierce and Morgan, 1992, Figure 10	0.125–4.5	2–10 Ma			
Grand Valley, ID	**14**	Piety *et al.*, 1992	1.8# 0.12–0.16	2–4.3 4.3–10 Ma			
Lost River, Arco, ID	Arco Segment, **15**	Pierce and Morgan, 1992, Figure 9	0.50 0.11 0.46 0.07	25–30 30–82 82–94 94–165	0.11	0.87	0.435 0.096 0.400 0.061
Sierra Nevada, June Lake area, CA	June Lake, **6**	Bursik and Sieh, 1989, Figure 4	0.50 0.96 0.91 1.61	0–16 ka 16–39 ka 39–72 ka 72–165 ka	1.26	0.079	0.040 0.076 0.072 0.127
Sierra Nevada, June Lake area, CA	Lundy Canyon, **16**	Bursik and Sieh, 1989, Figure 4	1.23 0.19	16–130 ka 130–750 ka	0.34	0.294	0.362 0.056
Sierra Nevada, June Lake area, CA	Bloody Canyon, **16**	Bursik and Sieh, 1989, Figure 4	0.92 0.67	60–130 130–200	0.78	0.128	0.118 0.086
Pitaycachi, Sonora, MEX	Pitaycachi, **17**	Bull and Pearthree, 1988	0.024 0.018 0.012	0–150 ka 150–350 ka 350–1000 ka	0.015	6.66	0.160 0.120 0.080
Lemhi, ID	Ellis Segment, **18**	Knuepfer and Baltzer, unpublished	0.21 0.10	6–20 ka 20–70 ka	0.13	0.77	0.162 0.077
Lemhi, ID	Big Gulch, **18** Segment	Knuepfer and Baltzer, unpublished	0.36 0.16	6–20 ka 20–70 ka	0.23	0.417	0.15 0.067

Statistics for normalized vertical slip rates: excluding Wasatch Fault data, $n = 28$, mean = 0.13 mm/yr, standard deviation = 0.10 mm/yr.

*Numbers in bold refer to locations shown on Figure 1.

**Vertical slip rate calculated from the increment of fault scarp height divided by the time period during which that height was created.

†Time period during which the increment of scarp height was created.

‡Total fault scarp height on the oldest datum divided by the age of that datum. This value also equals the weighted average of the slip rates for various time periods at each fault site.

§*N* factor = normalization factor, derived by dividing the long-term mean vertical slip rate into 0.1 mm/yr.

‖*N* slip rate = vertical slip rate for the given time period multiplied times the *N* factor for that fault.

¶Normalized slip rates from the Wasatch fault zone show anomalous amount of variation ($n = 8$, mean = 0.91 mm/yr, standard deviation = 1.38 mm/yr) and may be affected by fluctuations in adjacent Pleistocene Lake Bonneville. These data were not used in constructing the CDF.

#Slip rates for the Grand Valley fault cover a much longer time span (several My) than do other slip rates, and so they were not used in construction of the CDF.

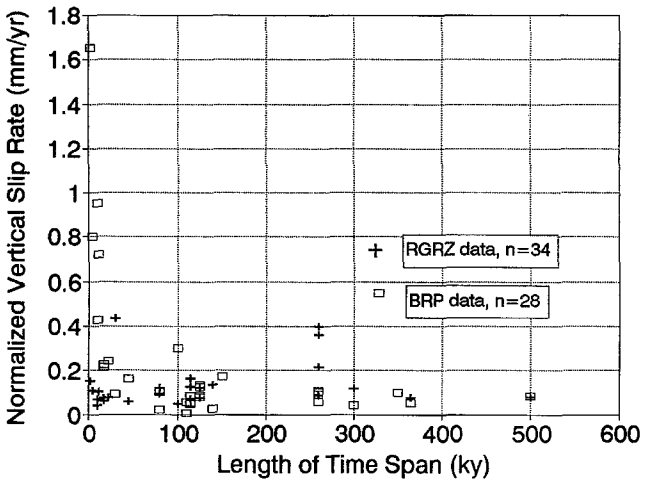

Figure 2. Normalized vertical slip rates for normal faults in the Rio Grande Rift Zone (RGRZ) and Basin and Range province (BRP) as a function of the length of time span inventoried (in ky, 1 ky = 1000 years). In general, the highest normalized slip rates are associated with the shortest time spans, but considerable variation occurs.

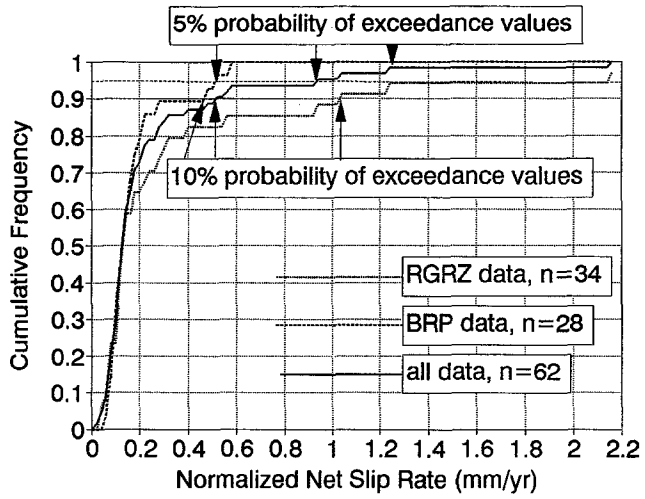

Figure 3. Cumulative density function (CDF) of normalized net slip rates for three data sets from the western United States. RGRZ = Rio Grande Rift Zone, BRP = Basin and Range province, all data = RGRZ and BRP data. The net slip rates in this diagram were computed from the vertical slip rates in Tables 1 and 2 by assuming a fault dip of 60° and multiplying vertical slip rates by 1.2. This conversion was performed so CDF values for net slip rate could be compared to net slip rates estimated by expert opinion (Woodward-Clyde, 1993). The 5% and 10% probability of exceedance values (i.e., 90% and 95% cumulative frequency values) are highlighted for each of the three data sets.

In contrast, the CDF suggests that the mean slip rate is not operative over much of the fault's life span and assigns a much higher probability to the highest slip rate considered by the panel (22% probability for 0.30 mm/yr). However, the branches in Figure 4b do not reflect the very high slip rates possible at the 10% and 5% probabilities of exceedance (Fig. 3). One way to reflect those values is to construct five tree branches with equal (20%) probabilities of occurrence (Fig. 4c), based on the all-fault data CDF in Figure 3 (see Fig. 4 caption for explanation of the method). The highest slip-rate category in such a scenario is 0.52 mm/yr (the 10% probability of exceedance value) and is much higher than any of the values chosen by the expert panel. Thus, it appears that the expert panel underestimated the amount of possible variance in slip rate over time, especially at low probability levels.

This analysis is admittedly simplistic and makes some questionable assumptions: (1) that slip-rate variability over time is the same for high slip rate normal faults (ca. 2 mm/yr) as for very low slip rate normal faults (ca. 0.01 mm/yr) and (2) that the ergodic substitution is warranted. However, we have no evidence to contradict either assumption at this point. The advantages of an inventory-based empirical procedure are that it is reproducible, that it results in a full cumulative density function for slip rate, and that it provides a quantitative basis for assigning slip rates and associated probabilities to a logic tree.

Acknowledgments

I thank Jeff Kimball (U.S. Department of Energy) for pointing out potential shortcomings in the expert panel conclusions and Ivan Wong (Woodward-Clyde Federal Services) for supporting this line of investigation. Susan Olig (WCFS) and Keith Kelson (Lettis & Assoc.) posed their usual probing questions. Mike Machette (U.S. Geological Survey) encouraged the writer to publish the results in a timely fashion and reviewed the article. Peter Knuepfer contributed unpublished data on the Lemhi Fault, Idaho. This article benefitted from reviews by Mike West and one anonymous reviewer.

References

Bull, W. B. and P. A. Pearthree (1988). Frequency and size of Quaternary surface ruptures of the Pitaycachi fault, northeastern Sonora, Mexico, *Bull. Seism. Soc. Am.* **78,** 956–978.

Bursik, M. and K. Sieh (1989). Range front faulting and volcanism in the Mono Basin, eastern California, *J. Geophys. Res.* **94,** 15587–15609.

Chorley, R. J., S. A. Schumm, and D. E. Sugden (1984). *Geomorphology,* Methuen, London, 605 pp.

Coppersmith, K. J. and R. R. Youngs (1986). Capturing uncertainty in probabilistic seismic hazard assessments within intraplate tectonic environments, *Proc. Third National Conference on Earthquake Engineering,* Charleston, South Carolina, **1,** 301–312.

dePolo, C. M. (1994). Estimating fault slip rates in the Great basin, USA, in *Proc. of the Workshop on Paleoseismology, U.S. Geol. Surv. Open-File Rept. 94-568,* 48–49.

Hunter, R. L. and C. J. Mann (Editors) (1992). Techniques for determining probabilities of geologic events and processes, *Int. Assoc. Math. Geol., Stud. Math. Geol.,* Vol. 4, Oxford Univ. Press, Oxford, UK, 364 pp.

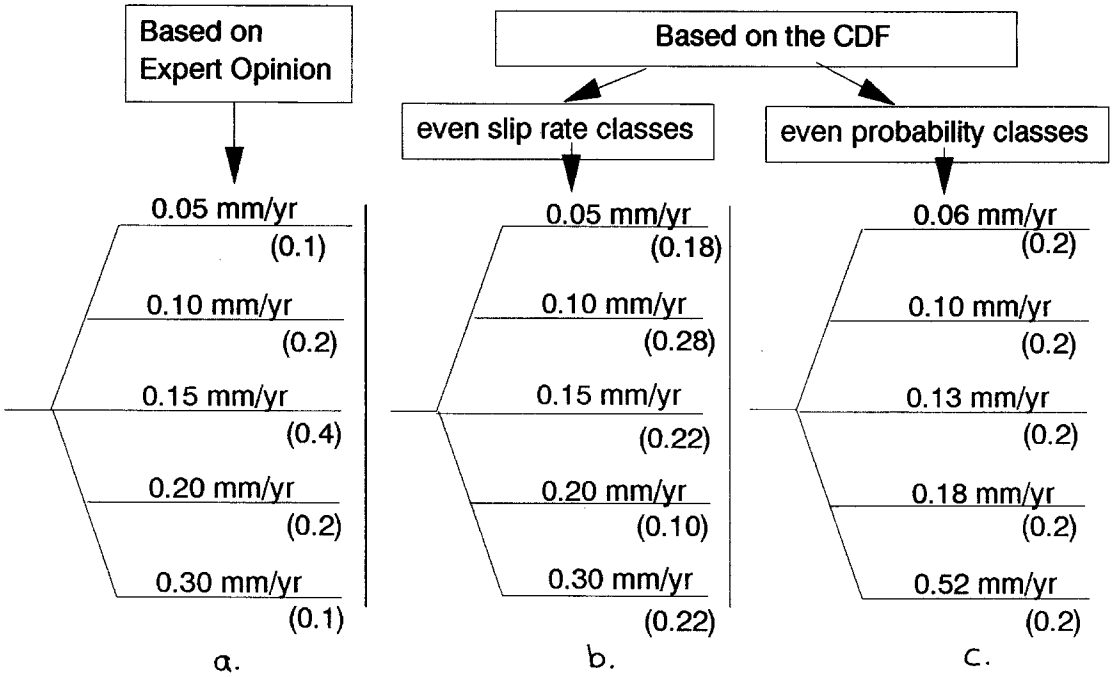

Figure 4. Schematic diagrams of part of a logic tree representing slip rates for the Pajarito fault zone. (a) Branch values as derived from a consensus of experts (Woodward-Clyde, 1993). (b) Branch values using the same slip-rate classes as part (a) but with probabilities derived from the CDF curve using all data. Note the increase in probability for the highest slip rate class and the decreased probability for classes near the median, compared to the expert opinion tree. (c) Slip-rate values adjusted to the midpoint of five classes of equal probability. Slip-rate values are equal to the 10%, 30%, 50%, 70%, and 90% cumulative frequency values from the all-data CDF curve. Note how much higher the highest slip rate and probability are compared to the expert opinion tree.

Machette, M. N. (1978). Dating Quaternary faults in the southwestern United States by using buried calcareous paleosols, *U.S. Geol. Surv. J. Res.* **6,** 369–381.

Machette, M. N. (1985). Late Cenozoic geology of the Beaver Basin, southwestern Utah: *Brigham Young Univ. Geol. Stud.* **32,** 9–37.

Machette, M. N. (1987a). Preliminary assessment of Quaternary faulting near Truth or Consequences, New Mexico, *U.S. Geol. Surv. Open-File Rept. 87-652,* 40 pp.

Machette, M. N. (1987b). Preliminary assessment of paleoseismicity at White Sands Missile range, southern New Mexico; evidence for recency of faulting, fault segmentation, and repeat intervals for major earthquakes in the region, *U.S. Geol. Surv. Open-File Rept. 87-444,* 46 pp.

Machette, M. N. (1988). Quaternary movement along the La Jencia fault, central New Mexico, *U.S. Geol. Surv. Prof. Paper 1440,* 82 pp.

Machette, M. N., S. F. Personius, and A. R. Nelson (1992). Paleoseismology of the Wasatch fault zone: a summary of recent investigations, interpretations, and conclusions, in *Assessment of Regional Earthquake Hazards and Risk Along the Wasatch Front, Utah,* P. L. Gori and W. W. Hays (Editors), *U.S. Geol. Surv. Prof. Paper 1500-A,* A1-A71.

Mayer, L. (1984). Dating Quaternary fault scarps in alluvium using morphological parameters, *Quaternary Res.* **22,** 300–313.

McCalpin, J. P. (1983). Quaternary geology and neotectonics of the west flank of the northern Sangre de Cristo Mountains, south-central Colorado, *Colorado School Mines Q.* **77,** no. 3, 97 pp.

McCalpin, J. P. (1993). Neotectonics of the northeastern Basin and Range margin, western USA, *Zeit. fur Geomorph., Suppl. Bd.* **94,** 137–157.

Menges, C. M. (1990). Late Quaternary fault scarps, mountain-front landforms, and Pliocene-Quaternary segmentation on the range-bounding fault zone, Sangre de Cristo Mountains, New Mexico, in *Neotectonics in Earthquake Evaluation, Rev. Engin. Geol.,* E. L. Krinitsky and D. B. Slemmons (Editors), Vol. VIII, Geol. Soc. Amer., Boulder, CO, 131–156.

Pierce, K. L. and L. A. Morgan (1992). The track of the Yellowstone hot spot, volcanism, faulting, and uplift, in *Regional Geology of Eastern Idaho and Western Wyoming, Geol. Soc. Am. Memoir,* P. K. Link *et al.* (Editors), **179,** 1–54.

Piety, L. A., J. T. Sullivan, and M. H. Anders (1992). Segmentation and paleoseismicity of the Grand Valley fault, southeastern Idaho and western Wyoming, in Link, P. K., Kuntz, M. A. and Platt, L. B. (eds.), *Regional Geology of Eastern Idaho and Western Wyoming: Geol. Soc. Am. Memoir,* P. K. Link, M. A. Kuntz, and L. B. Platt (Editors), **179,** 155–182.

Reiter, L. (1990). *Earthquake Hazard Analysis; Issues and Insights,* Columbia Univ. Press, New York, 254 pp.

Woodward-Clyde Federal Services (1993). Seismic hazards evaluation of the Los Alamos National Laboratory, unpublished Draft Final Report to Los Alamos National Laboratory, New Mexico, by Woodward-Clyde Federal Services, Oakland, California, 3 vols., 1 June, 1993.

GEO-HAZ Consulting, Inc.
343 S. Saint Vrain #4
Estes Park, CO 80517

Manuscript received 23 January 1995.